ISTITUTO NAZIONALE DI FISICA NUCLEARE

Sezione di Milano

INFN/TC–98/05
17 Febbraio 1998

E. Acerbi, G. Ambrosio, G. Baccaglioni, M. Sorbi, G. Volpini:

A NEW APPROACH FOR THE PROTECTION SYSTEM OF THE SUPERCONDUCTING COILS IN THE BARREL TOROID OF ATLAS

PACS: 85.25

Published by ***SIS–Pubblicazioni***
Laboratori Nazionali di Frascati

INFN – Istituto Nazionale di Fisica Nucleare
Sezione di Milano

INFN/TC–98/05
17 Febbraio 1998

A NEW APPROACH FOR THE PROTECTION SYSTEM OF THE SUPERCONDUCTING COILS IN THE BARREL TOROID OF ATLAS.

E. Acerbi, G. Ambrosio, G. Baccaglioni, M. Sorbi, G. Volpini
INFN – Sezione di Milano, Laboratorio LASA and Dipartimento di Fisica dell'Università di Milano, via fratelli Cervi 201, 20090 Segrate (MI), Italy

Abstract

An analysis of the discharge of the Barrel Toroid under several operating conditions has been carried out in order to verify the possibility of an improvement of the protection system of the superconducting coils and to program tests on the Bo coil.

The main critical parameters of the discharge (i.e. the maximum temperature inside the coils, the maximum temperature gradient, the maximum voltage at the coil ends and the maximum decentering forces acting on the BT and ECT magnets) have been calculated for several operating conditions (heaters on, heaters off, short circuit with heaters on or off).

The results of the analysis are the basis for the proposal of some improvements on the protection system of the Barrel Toroid.

1 INTRODUCTION

Normally the protection system of a superconducting magnet is designed in order to extract the energy stored in the magnetic field in a such way that:

a) the maximum temperature of the coil is limited to 100-120 K, to avoid damages to the insulation produced by stresses arising by high temperature gradients;

b) the maximum voltage is limited to a design value (tipically $\Delta V_{max} < 1000\,V$), determined by the insulation thickness (ground, interpancake and turn to turn insulation), in order to avoid the insulation breakage due to an arc in the dielectric.

When the energy extraction is obtained with an external dump resistor, the previous conditions are in conflict. In fact the first condition requires high dump resistance whereas the second one requires low dump resistance.

Generally a suitable design of the coil (number of turns and operating current), of the superconducting cable (cross section and residual resistivity ratio of the matrix) and of the dump resistor allows to satisfy both conditions.

In the case of the coils of the ATLAS Barrel Toroid an high level of protection has been adopted by reducing drastically the dump resistance and, as consequence, the maximum voltage at the ends of the coil (see [1]). This choice represents a safeguard against the effect of a short circuit during a fast discharge of the magnet. It is easy to show that high unbalanced currents install in the short-circuited coil, by producing high forces (mainly between the BT and ECT coils) that cannot be effectively opposed by the detector structure.

The main consequence of this choice is the necessity to induce a fast transition from the superconducting to the resistive state of all the coils by means of heaters (resistive or inductive) in order to avoid that the magnetic energy is dissipated in a limited region of the coils by producing too high temperatures and gradients. The analysis of the discharge process shows that, if the heaters work correctly, the coils quench completely in a few seconds and a temperature lower than $100\,K$ is reached almost homogeneously by all the coils.

If the heater system does not work, the magnetic energy could be dissipated almost completely in the coil in which a quench has been originated by causing the fast discharge. In this fault scenario the maximum temperature could approach the room temperature and the maximum voltage (inside the magnet) could be of 1000-1500 V.

Therefore the drastic reduction of the dump resistance (in order to limit the very negative effects of a short circuit) can produce, if the heaters do not work, the conditions for the birth of short circuits (helped by the high stresses and the high voltages during the magnet discharge).

The aim of the present study is to verify if there are more convenient solutions of the protection system that represent a reasonable safeguard against the failure of the heaters and against the danger of short circuits.

It is sure that it does not exist a miraculous solution that eliminates all the unwelcome effects of the fault scenario, but it is possible to choose a solution which minimizes the consequences of these events.

In this paper the presentation of a new approach for the protection system is preceded by the analysis of a fast discharge of the coils in the normal conditions and in presence of heater failure. Some sections are dedicated to the analysis of the short circuit scenario and the case of combined faults (heater failure and short circuit).

Finally the present and a new possible solution for the protection system are compared and the advantages and disadvantages of both solutions are discussed.

2 DISCHARGE OF THE BARREL TOROID COILS.

The study of the discharge of the coils requires, at the same time, an analysis of the electromagnetic processes (induction coupling with the other magnet components, short circuit) and of the thermal processes (quench propagation, heat exchange between the magnet components). Generally the electromagnetic processes are easily described by means of simple differential equations of coupled circuits whereas the thermal processes require a more complex treatment, often heavily computer time consuming. In fact the calculation of the temperature distribution in the coil and casing requires the solution of the heat propagation equations for a 3D geometry with distributed sources (heating of the casing due to the eddy currents) and localized sources (quenched portions of the coils) whose size and power are increasing in time.

In order to simplify the treatment of the thermal processes a few hypotheses have been introduced. These hypotheses, which are conservative for the coil protection, can be resumed in the following items:

- a) The coupling between the BT and the ECT coils and between the BT coils and the cryostat (thermal shields and vacuum vessels) are neglected. This means that the magnetic energy stored in the BT coils will be dissipated during a discharge only in the coils, the casing and the dump resistor.

- b) The quench (accidental or stimulated by heaters) propagates with constant speed both longitudinally and crosswise. The longitudinal speed v_x is used as a free parameter in the analysis whereas the transverse speeds v_y and v_z are linked to the previous one by the relations:

$$v_y = (\frac{k_y}{k_x})^{1/2} v_x \qquad\qquad v_z = (\frac{k_z}{k_x})^{1/2} v_x \tag{1}$$

  being k_x, k_y and k_z respectively the thermal conductivity of the matrix and the transverse thermal conductivities of the insulated coil. The evaluation of the quench speed for the ATLAS coils is carried out in the Appendix A.

- c) The temperature inside the quenched conductor is assumed constant and equal to the hot spot temperature and goes abruptly to the operating temperature of the magnet at the boundaries of the propagating zone. This assumption greatly simplifies the calculation and the resulting underevaluation of the spot temperature can be compensated, during the analysis, by a suitable reduction of the quench speed.

- d) The thermal exchanges between the coil and the casing can be considered or neglected (with an exchange factor varying from 1 to 0) . In the first case the efficiency of the quenchback for the coil safety can be evaluated. In the second case the worst situation for the coil safety can be simulated.

With these hypotheses the electromagnetic and thermal equations, which describe the coil discharge in the various operating conditions, are:

$$\frac{dI_1}{dt} = (\frac{1}{\alpha})[-L_2(R_d + r)I_1 + N_b M_{12} R_c I_2] \tag{2}$$

$$\frac{dI_2}{dt} = (\frac{1}{\alpha})[-L_1 R_c I_2 + M_{12}(R_d + r)I_1] \tag{3}$$

$$\frac{dT_x}{dt} = \frac{\rho_x I_1^2}{\delta_s c_x S_s^2} + \eta \frac{k_{is}(T_{m1})}{w_{is}\delta_s c_x h_c}(T_c - T_x) \tag{4}$$

$$\frac{dT_y}{dt} = f_1 \frac{\rho_y I_1^2}{\delta_s c_y S_s^2} + \eta \frac{k_{is}(T_{m2})}{w_{is}\delta_s c_y h_c}(T_c - T_y) \tag{5}$$

$$\frac{dT_c}{dt} = \frac{\rho_c I_2^2}{\delta_c c_c S_c^2} + \frac{\eta \Delta y}{w_{is}\delta_c S_c c_c}[k_{is}(T_{m1})(T_x - T_c)\frac{L_x}{L_c} + k_{is}(T_{m2})(T_y - T_c)\frac{L_y}{L_c}] \tag{6}$$

$$\frac{dT_d}{dt} = (\frac{1}{C_d})[R_d I_1^2 - Qe(T_d - T_o)] \tag{7}$$

where:

$$\alpha = L_1 L_2 - N_b M_{12}^2 \tag{8}$$

and:

I_1, I_2	current intensities in the BT coils and casings
T_x	temperature of the quenched zone of the coil
T_y	temperature of the remaining zone of the coil
T_c, T_d	temperature of the casing and dump resistor
L_1, L_2	self inductances of the toroid and casings
M_{12}	mutual inductance of 1 casing with the toroid
N_b	number of coils in the BT
R_d,R_c	resistances of the dump and a single casing
r	resistance of the quenched zone of the coil
ρ_x, c_x	resistivity and specific heat of the matrix at T_x
ρ_y, c_y	resistivity and specific heat of the matrix at T_y
ρ_c, c_c	resistivity and specific heat of the casing
δ_s,S_s	density and cross section of the conductor
δ_c,S_c	density and cross section of the casing
w_{is},k_{is}	thickness and thermal conductivity of the insulation
T_{m1},T_{m2}	$T_{m1} = (T_c + T_x)/2$ $T_{m2} = (T_c + T_y)/2$
Δy, h_c	width (short side) and height of the conductor
L_x	length of the quenched zone of the pancake
L_y	length of the superconducting or quenched back zone in the pancake
L_c	average length of the casing
η	reduction factor of the heat exchange between coil and casing
f_1	$f_1 = 0$ when $T_y < T_{crit}$ $f_1 = 1$ when $T_y > T_{crit}$
Q	flow of the cooling water in the dump
e	specific heat exchange
T_o	inlet temperature of the water
C_d	thermal capacity of the dump resistor

The equations (2) and (3) describe the electromagnetic coupling between the coils and the casings during the discharge. The self and the mutual inductances are constant (see [2]) whereas the dump, coil and casing resistances are variable because of the heating and the quench propagation. These quantities are calculated at every integration step.

The equation (4) and (5) describe the temperature behaviour in the regions reached by the accidental or stimulated quench and in the regions not yet directly reached by the quench. In other words the equation (4) is connected with the direct propagation of the quench (T_x represents the hot spot temperature), whereas the equation (5) is connected with the quenchback (eddy currents and heat exchange in the casing) and T_y represents the constant temperature of the superconducting or quenchedback conductor.

Because the equation (4) and (5) contain steady state terms, concerning the heat exchange between the coil and the casing, they don't give an exact representation of the process. Nevertheless because the discharge process is rather slow (about one hundred seconds) whereas the heat diffusivity time in the casing is short, this approximation does not disturb significantly the results and allows a comparison between different operating conditions.

The equations (6) and (7) describe respectively the temperature behaviour of the casing and the dump resistor.

The lengths L_x and L_y, as a function of time, depend by several parameters (quench speed, coil geometry, position of the starting quench). The hypoteses for the calculation and the resulting expressions of L_x are presented in the Appendix B. The length L_y is simply given by:

$$L_y = L_{tot} - L_x \tag{9}$$

where L_{tot} is the total length of the conductor in a BT coil.

The values of the casing and dump resistances, as a function of time (or temperature) are easily obtained by the material properties. The resistance $r(t)$ of the quenched cable is obtained as:

$$r(t) = (\frac{1}{S_s})(\rho_x L_x + f_1 \rho_y L_y) \tag{10}$$

The integration of the equations (2) - (7) has been obtained by means of the Runge Kutta method.

3 ANALYSIS OF THE BT DISCHARGE IN NORMAL AND FAULTY CONDITIONS.

The behaviour of the coil discharge has been analyzed as a function of the quench speed and the dump resistance for different operating conditions:

- Normal conditions: heaters full operating with and without heat exchange between coil and casing.
- Faulty conditions: heaters not operating with and without heat exchange between coil and casing.

The effects of a short circuit during the discharge in the normal operating conditions and in concomitance of heater failure will be examined in the next section.

The parameters that have been considered to evaluate the riskiness for the coil safety are:

- the hot spot temperature in the coil (T_{max}),
- the maximum voltage (at the coil ends) (V_{max}) and the current intensity (I_1) at the maximum voltage,

- the maximum temperature difference between coil and casing (ΔT),
- the delay between the start of the discharge and the beginning of the quenchback (Δt).

Additional parameters considered in the analysis are the maximum current in the casing (I_{2m}) and the ratio (ϵ) between the energy dissipated in the magnet (coils and casings) and the total magnetic energy.

The data of the analysis for different operating conditions are reported in Tables C1 - C6 of the Appendix C.

In the following paragraphs of this section the main results and some preliminary conclusions will be presented.

3.1 Discharge in normal conditions.

The typical behaviours of the current intensities in the coil and in the casing during a normal fast discharge respectively on a dump resistance of $2\,m\Omega$ and $20\,m\Omega$, in the worst case (low quench speed and no heat exchange between the casing and coil) are shown in Fig. 1.

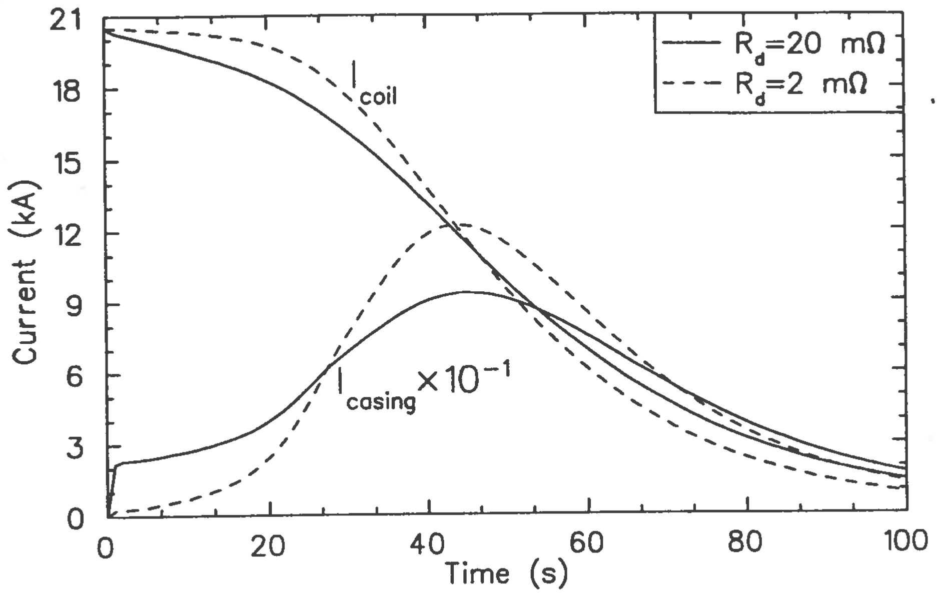

FIG. 1: Current intensities of the coils and casing during a normal fast discharge in the worst case ($v_x = 1\,m/s$ and no heat exchange between casing and coil).

Fig. 2 shows the evolution of the coil and casing temperatures for the same operating conditions.

From the data, reported in Tables C1-C6, and from the previous figures the following results have been obtained:

- The hot spot temperature is always lower than $100\,K$ and it is not very dependent on the quench speed, the dump resistance and the level of heat exchange between the casing and the coil. The hot spot temperature goes from $T_{max} = 86.3\,K$ (no heat exchange with the casing, very low quench speed and very low dump resistance) to $T_{max} = 67.5\,K$ (with a normal heat exchange, high quench speed and high dump resistance).

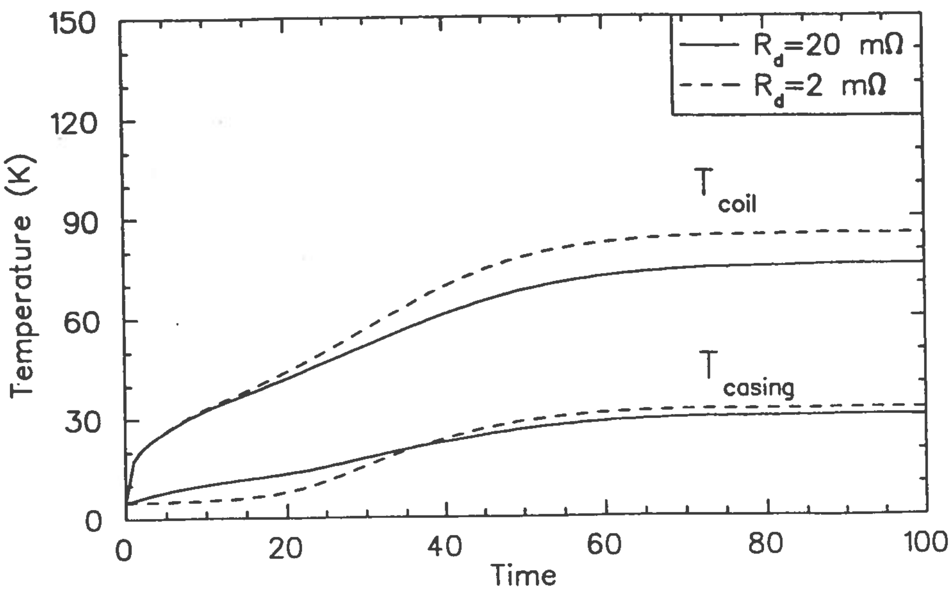

FIG. 2: Evolution of the coil and casing temperatures during a normal fast discharge in the worst case ($v_x = 1\,m/s$ and no heat exchange between casing and coil).

- The maximum voltage at the magnet ends is varying from about $10\,V$ (when $R_d = 0.2\,m\Omega$) to about $400\,V$ (when $R_d = 20\,m\Omega$) and the voltage is uniformly distributed inside the coils.
- The quenchback (due to the heating of the casing and the heat exchange with the coils) is operating in a few seconds (Δt ~3-18 s mainly depending by the quench speed) but it has not a significant impact on the reduction of the hot spot temperature. It can be considered an efficient safeguard for the magnet safety in case of heater failure.
- The maximum temperature drop between the coil and the casing is about $53\,K$ (when no heat exchange between the last ones and a very low dump resistance are considered) and about $26\,K$ (when a normal heat exchange and high dump resistance are considered). These temperature drops produce additional pressures, respectively of $3.5\,MPa$ and $1.4\,MPa$ on the conductor, insulation and bladders, that can be easily supported by the materials.

From this analysis it seems that in normal conditions the only advantage to use an high dump resistance (with an upper limit of $20\,m\Omega$ in order to maintain the voltage at the coils ends lower than $500\,V$) is that about 30% of the magnet energy is dissipated outside. This means a reduced consumption of refrigerant and a faster cooling of the magnet after a discharge (saving of about 30% of cost and cooling time).

3.2 Discharge with heater failure.

The typical behaviours of the current intensities in the coil and casing during a fast discharge, respectively on a dump resistance of $2\,m\Omega$ and $20\,m\Omega$, in the worst case (heater failure, high speed of the initial quench and no heat exchange between the casing and coil) are shown in Fig. 3.

Fig. 4 shows the evolution of the coil and casing temperatures for the same operating conditions.

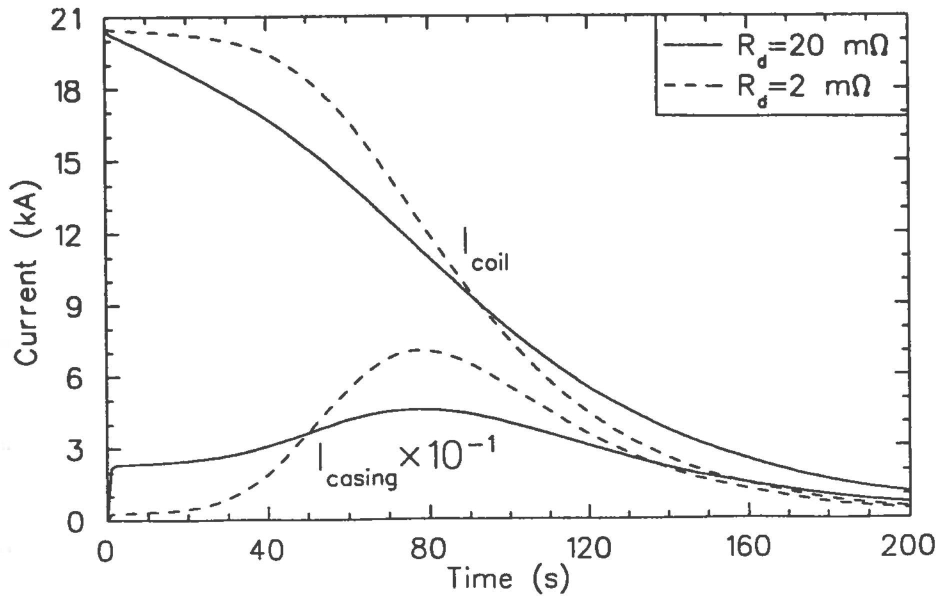

FIG. 3: Current intensities of the coils and casing during a faulty fast discharge in the worst case ($v_x = 1\,m/s$ and no heat exchange between casing and coil).

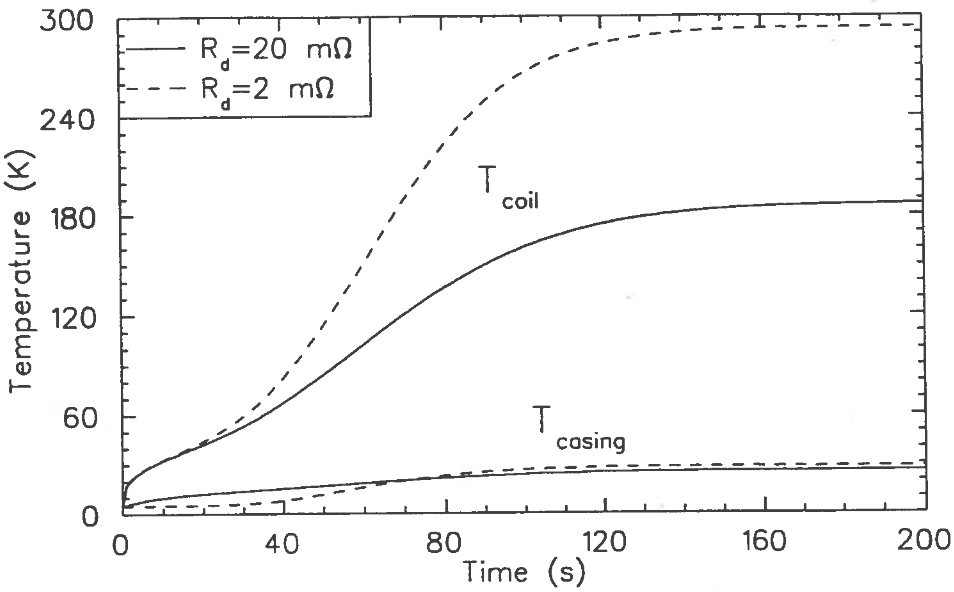

FIG. 4: Evolution of the coil and casing temperatures during a faulty fast discharge in the worst case ($v_x = 1\,m/s$ and no heat exchange between casing and coil).

Table I summarizes the main parameters (T_{max}, V_{max}, ΔT and ϵ) of the discharge on the dump resistances ($R_d = 2\,m\Omega$ and $R_d = 20\,m\Omega$) for the worst case (no heat exchange) and more realistic cases (low and normal heat exchange).

The data of Table I show that in faulty conditions the high dump resistance and the quench back have a beneficial effect on the the hot spot temperature, the maximum voltage at the coil ends and the temperature drop between coil and casing.

It is clear that in the case of heater failure it is mandatory that the coil have a good thermal contact with the casing, otherwise the risk of irreversible damages to the coil becomes very high.

It is also clear that the dangerous effects of the high temperatures and voltages can be drastically reduced if an high dump resistance is used in the discharge circuit.

Table I
Parameters of the discharge with heater failure

Condition	R_d $(m\Omega)$	T_{max} (K)	V_{max} (V)	ΔT (K)	ϵ $(\%)$
No heat	2	294	1084	266	93.2
exchange	20	187	431	162	42.7
Low heat	2	245	863	196	93.4
exchange	20	116	107	77	54.3
Norm. heat	2	198	614	133	93.3
exchange	20	88	-59	42	54.5

Furthermore, with the high dump resistance, the energy extracted by the magnet is about 55% (instead of only 7%) with obvious advantages.

Another advantage, if the $20\,m\Omega$ dump resistance solution is adopted, is that the quenchback can replace the heaters when the discharge occurs at intermediate current intensities between the maximum ($I_{max} = 20500\,A$) and the lowest dangerous value ($I = 20500/(8)^{1/2}\,A$). In fact in this current range (mainly near the lowest value) the heaters can become less effective or completely ineffective so that a rapid process of quenchback can maintain within acceptable values the maximum voltage and the maximum temperature in the coil. The efficiency of the quenchback, when the high dump resistance is used, is clearly shown in Fig. 3 where the induced current in the casing jumps in 1 or 2 seconds to about 25000 A whereas with the low dump resistance the induced current is ten times lower.

These conclusions must be re-examined after the analysis of the effects of a short circuit in the coil with and without heater failure.

4 DISCHARGE IN PRESENCE OF A SHORT CIRCUIT.

In order to determine the role played by the various components of the magnet in the behaviour of the fast discharge, when a short circuit occurs, the problem has been faced in two steps:

- Only thermal (heat exchange) and no electromagnetic coupling between the coils and casings has been considered. In this case the problem can be described by only 7 differential equations (2 for the current intensities in the two BT sections, 4 for the temperatures of two reference coils and casings and 1 for the dump resistor temperature).

- Both thermal and electromagnetic couplings between the coils and casings have been considered. In order to simplify the treatment of the problem it has assumed that the current intensities in the casings of each BT section are the same. With this assumption the analysis of the discharge requires 13 differential equations (4 for the current intensities in the reference coils and casings in the two sections, 8 for the coils and casings temperatures and 1 for the dump resistor temperature).

4.1 First step analysis.

The scheme of the electrical circuit in this case is shown in Fig. 5.

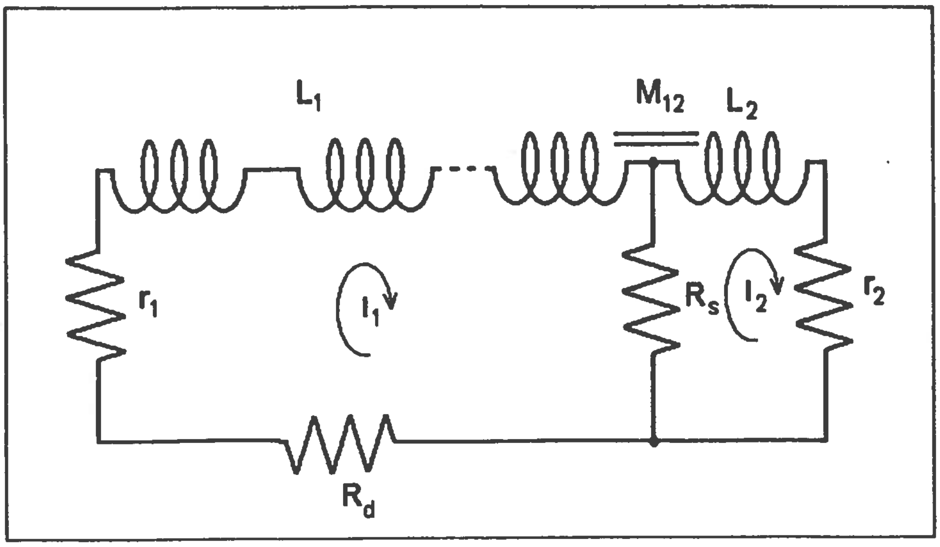

FIG. 5: Electrical scheme of the short circuited coils without electromagnetic coupling between coils and casings.

The electrical behaviour of the magnet is described by the following system of differential equations:

$$0 = L_1\frac{dI_1}{dt} + M_{12}\frac{dI_2}{dt} + R_s(I_1 - I_2) + (R_d + r_1)I_1 \quad (11)$$

$$0 = L_2\frac{dI_2}{dt} + M_{12}\frac{dI_1}{dt} + R_s(I_2 - I_1) + r_2 I_2 \quad (12)$$

where:

L_1	self inductance of the section without short circuit
L_2	self inductance of the section with short circuit
M_{12}	mutual inductance between the coils of the two sections
I_1,I_2	current intensities in the two BT sections
r_1,r_2	resistances of the quenched zones of the two BT sections
R_s	the resistance of the short circuit
R_d	the resistance of the dump

This system of equations must be completed by the thermal equations describing the evolution of the temperatures in the coils and casings. The complete set of equation is given by:

$$\frac{dI_1}{dt} = (\frac{1}{\alpha_s})\{[\beta_2 R_s + M_{12}r_2]I_2 - [\beta_2 R_s + L_2(R_d + r_1)]I_1\} \quad (13)$$

$$\frac{dI_2}{dt} = (\frac{1}{\alpha_s})\{-[\beta_1 R_s + L_1 r_2]I_2 + [\beta_1 R_s + M_{12}(R_d + r_1)]I_1\} \quad (14)$$

$$\frac{dT_1}{dt} = f_1\frac{\rho_1 I_1^2}{\delta_s c_1 S_s^2} + \eta\frac{k_{is}(T_{m1})}{w_{is}\delta_{is}c_1 h_c}(T_{c1} - T_1) \quad (15)$$

$$\frac{dT_2}{dt} = f_2\frac{\rho_2 I_2^2}{\delta_s c_2 S_s^2} + \eta\frac{k_{is}(T_{m2})}{w_{is}\delta_{is}c_2 h_c}(T_{c2} - T_1) \quad (16)$$

$$\frac{dT_{c1}}{dt} = \eta\frac{\Delta y}{w_{is}\delta_c S_c c_c}[k_{is}(T_{m1})(T_1 - T_{c1})\frac{L_{x1}}{L_c}] \quad (17)$$

$$\frac{dT_{c2}}{dt} = \eta\frac{\Delta y}{w_{is}\delta_c S_c c_c}[k_{is}(T_{m2})(T_2 - T_{c2})\frac{L_{x2}}{L_c}] \quad (18)$$

$$\frac{dT_d}{dt} = \frac{1}{C_d}[R_d I_1^2 - Qe(T_d - T_o)] \quad (19)$$

where:

$$\alpha_s = L_1 L_2 - M_{12} \quad (20)$$

$$\beta_1 = L_1 + M_{12} \quad (21)$$

$$\beta_2 = L_2 + M_{12} \quad (22)$$

and:

T_1,T_2	temperatures of the quenched zones in the two BT sections
T_{c1},T_{c2}	temperatures of the reference casings in the two BT sections
T_{m1}, T_{m2}	$T_{m1} = (T_1 + T_{c1})/2 \qquad T_{m2} = (T_2 + T_{c2})/2$
ρ_1, ρ_2	resistivity of the matrix in the reference coils of the two BT sections
c_1, c_2	specific heat of the matrix in the two BT sections
L_{x1},L_{x2}	lengths of the quenched zone in the reference coils of the two BT sections

The parameters f_1, f_2 are used to describe the various operating conditions:

- $f_1 = f_2 = 1$ when the heaters are on,
- $f_1 = 1$, $f_2 = 0$ when the heaters are off and the quench is in the first section of the magnet (unshorted section),
- $f_1 = 0$, $f_2 = 1$ when the heaters are off and the quench is in the second section of the magnet (shorted section).

The other parameters have the same meaning already defined in the equations (2-7).

In the equations (15-18) the heat exchange between the superconducting or quenched back zone of the coil and the corresponding casing has been neglected because it is active only in the first instants of the discharge and it does not modify substantially the evolution of the process.

4.2 Second step analysis

The scheme of the electrical circuit in this case is shown in Fig. 6.

By assuming that the casings of each BT section have the same current intensity (respectively I_3 and I_4) and neglecting the coupling between coil and casing of different

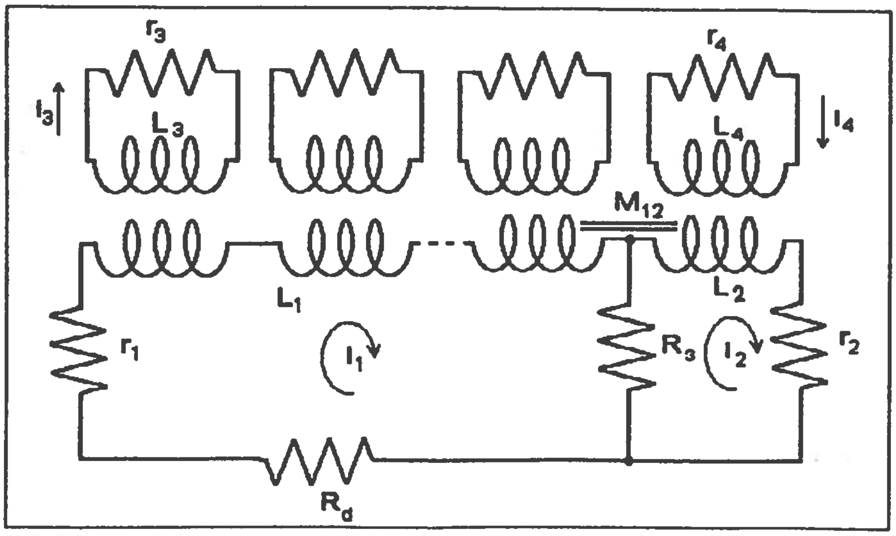

FIG. 6: Electrical scheme of the short circuited coils with electromagnetic coupling between coils and casings.

sections, the electrical equations describing the magnet discharge are:

$$0 = L_1\frac{dI_1}{dt} + M_{12}\frac{dI_2}{dt} + M_{13}\frac{dI_3}{dt} + (R_d + r_1)I_1 + R_s(I_1 - I_2) \quad (23)$$

$$0 = L_2\frac{dI_2}{dt} + M_{21}\frac{dI_1}{dt} + M_{24}\frac{dI_4}{dt} + r_2 I_2 + R_s(I_2 - I_1) \quad (24)$$

$$0 = L_3\frac{dI_3}{dt} + M_{31}\frac{dI_1}{dt} + r_3 I_3 \quad (25)$$

$$0 = L_4\frac{dI_4}{dt} + M_{42}\frac{dI_2}{dt} + r_4 I_4 \quad (26)$$

where:

L_1, L_2	self inductances of the first (unshorted) and second (shorted) section
L_3, L_4	self inductance of the reference casings in the first and second section
M_{12}	mutual inductance between the two coil sections ($M_{12} = M_{21}$)
M_{13}	mutual inductance of the coils of the first section and all casings of the first section
M_{31}	mutual inductance of a single casing of the first section and the coils of the first section
M_{24}	mutual inductance of the coils of the second section and all casings of the second section
M_{42}	mutual inductance of a single casing of the second section and the coils of the second section
r_1,r_2	resistances of the quenched zone of the first and second section
r_3,r_4	resistances of the reference casings of the first and second section

I_1, I_2	current intensities in the two BT sections
I_3, I_4	current intensities in the reference casings of the two BT sections

The complete set, including the thermal equations, becomes:

$$\frac{dI_1}{dt} = (\gamma_1 - \frac{\beta_1}{\beta_2}\gamma_2)/(\alpha_1 - \frac{\beta_1}{\beta_2}\alpha_2) \quad (27)$$

$$\frac{dI_2}{dt} = [\gamma_2 - \alpha_2\frac{dI_1}{dt}]/\beta_2 \quad (28)$$

$$\frac{dI_3}{dt} = (-R_{c1}I_3 - M_{31}\frac{dI_1}{dt})/L_3 \quad (29)$$

$$\frac{dI_4}{dt} = (-R_{c2}I_4 - M_{42}\frac{dI_2}{dt})/L_4 \quad (30)$$

$$\frac{dT_{11}}{dt} = f_{11}\frac{\rho_{11}I_1^2}{\delta_s c_{11}S_s^2} + \eta\frac{k_{11}(T_{31} - T_{11})}{w_{is}\delta_s c_{11}h_s} \quad (31)$$

$$\frac{dT_{12}}{dt} = f_{12}\frac{\rho_{12}I_1^2}{\delta_s c_{12}S_s^2} + \eta\frac{k_{12}(T_{32} - T_{12})}{w_{is}\delta_s c_{12}h_s} \quad (32)$$

$$\frac{dT_{21}}{dt} = f_{21}\frac{\rho_{21}I_2^2}{\delta_s c_{21}S_s^2} + \eta\frac{k_{21}(T_{41} - T_{21})}{w_{is}\delta_s c_{21}h_s} \quad (33)$$

$$\frac{dT_{22}}{dt} = f_{22}\frac{\rho_{22}I_2^2}{\delta_s c_{22}S_s^2} + \eta\frac{k_{22}(T_{42} - T_{22})}{w_{is}\delta_s c_{22}h_s} \quad (34)$$

$$\frac{dT_{31}}{dt} = \frac{\rho_{31}I_3^2}{\delta_c c_{31}S_c^2} + \eta\frac{k_{11}(T_{11} - T_{31})L_{x1}}{w_{is}\delta_c S_c L_c c_{31}} \quad (35)$$

$$\frac{dT_{32}}{dt} = \frac{\rho_{32}I_3^2}{\delta_c c_{32}S_c^2} + \eta\frac{k_{12}(T_{12} - T_{32})L_{x2}}{w_{is}\delta_c S_c L_c c_{32}} \quad (36)$$

$$\frac{dT_{41}}{dt} = \frac{\rho_{41}I_4^2}{\delta_c c_{41}S_c^2} + \eta\frac{k_{21}(T_{21} - T_{41})L_{y1}}{w_{is}\delta_c S_c L_c c_{41}} \quad (37)$$

$$\frac{dT_{42}}{dt} = \frac{\rho_{42}I_4^2}{\delta_c c_{42}S_c^2} + \eta\frac{k_{22}(T_{22} - T_{42})L_{y2}}{w_{is}\delta_c S_c L_c c_{42}} \quad (38)$$

$$\frac{dT_d}{dt} = (\frac{1}{C_d})(R_d I_1^2 - Qe(T_d - T_o)) \quad (39)$$

where:

$$\alpha_1 = L_1 - M_{13}M_{31}/L_3 \quad (40)$$

$$\alpha_2 = \beta_1 = M_{12} \quad (41)$$

$$\beta_2 = L_2 - M_{24}M_{42}/L_4 \quad (42)$$

$$\gamma_1 = M_{13}r_3I_3/L_3 - (R_d + r_1 + R_s)I_1 + R_sI_2 \quad (43)$$

$$\gamma_2 = M_{24}r_4I_4/L_4 - (r_2 + R_s)I_2 + R_sI_1 \quad (44)$$

and:

T_{11} ,T_{12}	temperatures of the resistive coil and superconducting (or quenched back) coils in the first section (unshorted one)
T_{21} ,T_{22}	temperatures of the resistive coils and superconducting (or

	quenched back) coils in the second section (shorted one)
T_{31} ,T_{32}	temperatures of the casings of the resistive and superconducting coils in the first section
T_{41} ,T_{42}	temperatures of the casings of the resistive and superconducting coils in the second section
c_{11},c_{12}	specific heat of the first section coils
c_{21},c_{22}	specific heat of the second section coils
c_{31},c_{32}	specific heat of the first section casings
c_{41},c_{42}	specific heat of the second section casings

The parameters f_{11}, f_{12}, f_{21}, f_{22} are used to describe the various operating conditions:

- $f_{11} = 1$ when the heaters are on and, if the heaters are off, when $T_{11} > T_{crit}$ or the quench is in the first section. Otherwise $f_{11} = 0$.
- $f_{12} = 1$ when the heaters are on and, if the heaters are off, when $T_{12} > T_{crit}$. Otherwise $f_{12} = 0$.
- $f_{21} = 1$ when the heaters are on and, if the heaters are off, when $T_{21} > T_{crit}$ or the quench is in the second section. Otherwise $f_{21} = 0$.
- $f_{22} = 1$ when the heaters are on and, if the heaters are off, when $T_{22} > T_{crit}$. Otherwise $f_{22} = 0$.

The meaning of the other parameters can be easily deduced by the definitions contained in the previous analysis.

4.3 Analysis of the discharge with different operating conditions.

The critical parameter of the BT discharge in presence of a short circuit is represented by the current unbalance between the unshorted and shorted sections. In fact the current unbalance produces transversal forces on the BT coils and radial forces on the ECT magnets that can reach, depending by the operating conditions, unsupportable intensities.

These forces, evaluated in another paper (see [3]), depend by the current unbalance ΔI_{BT} and by the current I_x in the unshorted or shorted BT sections (or in the ECT magnet) and can be expressed simply by:

$$F_x = k_x I_x \Delta I_{BT} \tag{45}$$

where F_x is the transversal maximum force acting on a single coil of the BT or the total radial force acting on the ECT and k_x a factor depending by the toroid (BT or ECT) and its geometry.

The aim of the analysis is to find the time evolution of these forces and the operating conditions responsible of their highest intensities.

The calculation of the current unbalance, and as consequence of the forces on the BT and ECT magnets, depends by several variables:

- assumptions (electromagnetic or no electromagnetic coupling between coils and casings);

- short circuit configurations (1 to 7 short circuited coils);
- operating conditions (heaters on or heaters off);
- discharge parameters (dump resistance, heat echange between coils and casings, time delay between quench start and breaker opening, quench speed, place of the initial quench inside the unshorted or shorted section);

so that a complete analysis should require more than 3000 code runs.

For this reason, by considering that the current unbalance is a smooth function of the discharge parameters, the following procedure has been adopted:

- a) Analysis of the current unbalance, in the hypothesis of no electromagnetic coupling and normal operation of the heaters, for a limited subsystem of the above mentioned variables in order to find the worst operating condition (i.e. the maximum of the decentering forces acting in the toroids). Completion of the analysis only for the worst operating condition determined in the previous step.
- b) Analysis for the case of heater failure with the same procedure illustrated in the point a).
- c) Completion of the analysis by considering the electromagnetic coupling between coils and casings.

4.3.1 Normal operation of the heaters.

In this analysis a $2\,m\Omega$ dump resistor, a normal thermal exchange between the coils and casings, a quench speed of $3\,m/s$, a delay of $2\,s$ between the quench start and breaker opening and a zero short circuit resistance have been assumed. Furthermore it has been assumed that the ECT coils start the discharge at the same time of BT ones, with a time constant $\tau = 500\,s$ (conservative hypothesis).

In Figs. 7 and 8 the typical behaviour of the current in the two magnet sections (7-1 short circuit configuration, i.e. 7 unshorted coils and 1 shorted coil) and the forces acting on the BT and ECT coils, due to the current unbalance, are presented.

The Figs 7 and 8 show the behaviour of the BT and ECT forces when the initial quench is located respectively in the unshorted section and in the shorted one.

The main features that can be deduced by these graphs are:

- The maximum in the forces is reached after a few tens of seconds from the beginning of the discharge. Therefore there is reasonable time (a few seconds) for an intervention of the protection system.
- The forces can have opposite directions, depending by the place of the initial quench (unshorted or shorted section). The supports, that transmit these forces from the cold mass to the warm voussoirs must be designed accordingly.
- The forces are within a few tens of tons (comparable to the cold mass weigth of each BT coil or each ECT magnet), so that suitable supports can be designed without big problems of interferences with the other components of the detector.

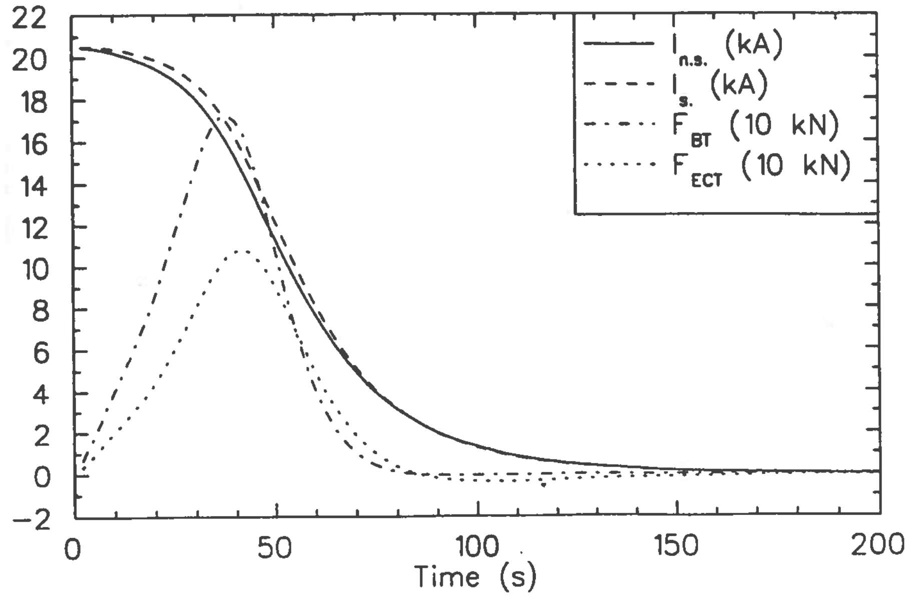

FIG. 7: Behaviour of the current in the unshorted (n.s.) and shorted (s.) BT sections and forces (absolute values) in the BT and ECT coils with a $2\,m\Omega$ dump resistor, heaters on and initial quench in the unshorted section.

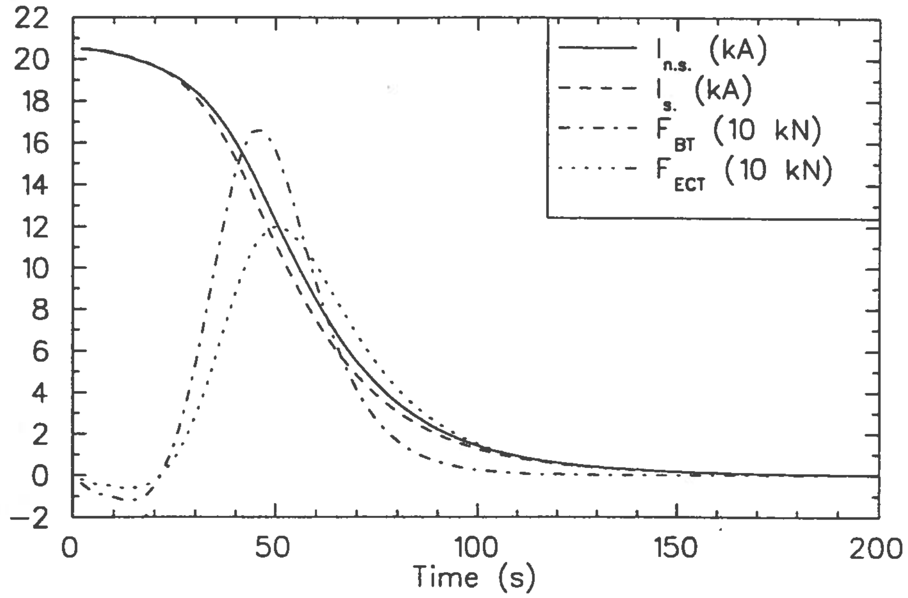

FIG. 8: Behaviour of the current in the unshorted (n.s.) ans shorted (s.) BT sections and forces (absolute values) in the BT and ECT coils with a $2\,m\Omega$ dump resistor, heaters on and initial quench in the shorted section.

The same force behaviour, illustrated in Figs 7 and 8, is present in each short circuit configuration. For this reason in Table II only the maximum of the forces in the ECT and BT are reported for the following situations:

- different short circuit configurations (seven);
- $2\,m\Omega$ and $20\,m\Omega$ dump resistance.

The positive or negative sign means that the absolute maximum force is reached when the initial quench is respectively inside the unshorted section (positive sign) or inside the shorted section (negative sign).

Table II - Forces in the BT and ECT coils (No e.m. coupling - Heaters on)

	$2\,m\Omega$		$20\,m\Omega$	
N_{ns}-N_s	F_{BT} (kN)	F_{ECT} (kN)	F_{BT} (kN)	F_{ECT} (kN)
7-1	+174	-120	+531	+321
6-2	+202	-221	+678	+648
5-3	+220	-295	+905	+971
4-4	+242	-332	+1131	+1257
3-5	+256	-332	+1381	+1486
2-6	+ 294	-298	+1656	+1590
1-7	+398	-240	+1147	+1399

When the dump resistance is $2\,m\Omega$, the worst situation for the forces on the BT ($F_{BT} \sim 41\,tons$) occurs with the 1-7 short circuit configuration, whereas for the force on the ECT ($F_{ECT} \sim 34\,tons$) occurs with the 4-4 short circuit configuration. Furthermore the maximum forces on the BT and ECT become 4-5 times higher when the dump resistance passes from $2\,m\Omega$ to $20\,m\Omega$: the maximum of the forces occurs with the 2-6 short circuit configuration ($F_{BT} \sim 169\,tons$ and $F_{ECT} \sim 162\,tons$).

It is clear from these data that, if the dump resistance of $20\,m\Omega$ will be chosen for the advantages illustrated in the previous paragraphs, it is necessary to use a different strategy for the protection of the coils, in order to avoid decentering forces higher than $50\,tons$.

For the second step of the analysis the 1-7 and the 4-4 short circuit configurations have been examined by varying the following parameters:

- time delay between quench start and breaker opening
- quench speed
- heat exchange between coils and casings.

The results show that the forces are very small dependent by the heat exchange between the coils and casings and by the quench speed whereas they are strongly dependent by the delay between the quench start, its detection and breaker activation. The data for different delays and two extreme quench speeds ($v_x = 1\,m/s$ and $v_x = 10\,m/s$) are reported in Table III and Table IV.

These results show that the load bearing structure for the BT coils and the ECT magnet must be designed to support at least 50 tons in order to accept a delay of 3-4 s between quench start and the breaker opening and to accept eventual dissymmetries in the quench propagation in the two sections of the BT.

4.3.2 Heater failure.

The behaviour of the current unbalance and decentering forces, in case of heater failure, 7-1 short circuit configuration and same parameters fixed in the previous subsection, is illustrated in Figs 9 and 10.

Table III - Forces in the BT and ECT coils as a function of the delay and quench speed for the 4-4 short circuit configuration (No e.m. coupling - Heaters on).

	$2\,m\Omega$				$20\,m\Omega$			
	$v_x = 1\,m/s$		$v_x = 10\,m/s$		$v_x = 1\,m/s$		$v_x = 10\,m/s$	
Delay (s)	F_{BT} (kN)	F_{ECT} (kN)	F_{BT} (kN)	F_{ECT} (kN)	F_{BT} (kN)	F_{ECT} (kN)	F_{BT} (kN)	F_{ECT} (kN)
0.0	+121	+131	109	+121	+1167	+1255	+1054	+1174
0.5	+141	+154	+132	-156	+1176	+1266	+1067	+1190
1.0	+168	-239	+161	-205	+1189	+1279	+1081	+1206
2.0	+251	-374	+238	-323	+1216	+1310	+1113	+1244
5.0	+620	-850	+545	-726	+1339	+1459	+1242	+1402
10.0	+1344	-1663	+1165	+1463	+1718	+1918	+1600	+1833

Table IV - Forces in the BT and ECT coils as a function of the delay and quench speed for the 2-6 short circuit configuration (No e.m. coupling - Heaters on).

	$2\,m\Omega$				$20\,m\Omega$			
	$v_x = 1\,m/s$		$v_x = 10\,m/s$		$v_x = 1\,m/s$		$v_x = 10\,m/s$	
Delay (s)	F_{BT} (kN)	F_{ECT} (kN)	F_{BT} (kN)	F_{ECT} (kN)	F_{BT} (kN)	F_{ECT} (kN)	F_{BT} (kN)	F_{ECT} (kN)
0.0	+376	-209	+338	-179	+1179	+1450	+1134	+1381
0.5	+386	-223	+350	-191	+1179	+1451	+1134	+1382
1.0	+396	-239	+364	-203	+1179	+1452	+1135	+1384
2.0	+423	-275	+393	-232	+1179	+1455	+1135	+1387
5.0	+545	-408	+509	-339	+1180	+1463	+1136	+1398
10.0	+800	-663	+740	-558	+1181	+1489	+1139	+1429

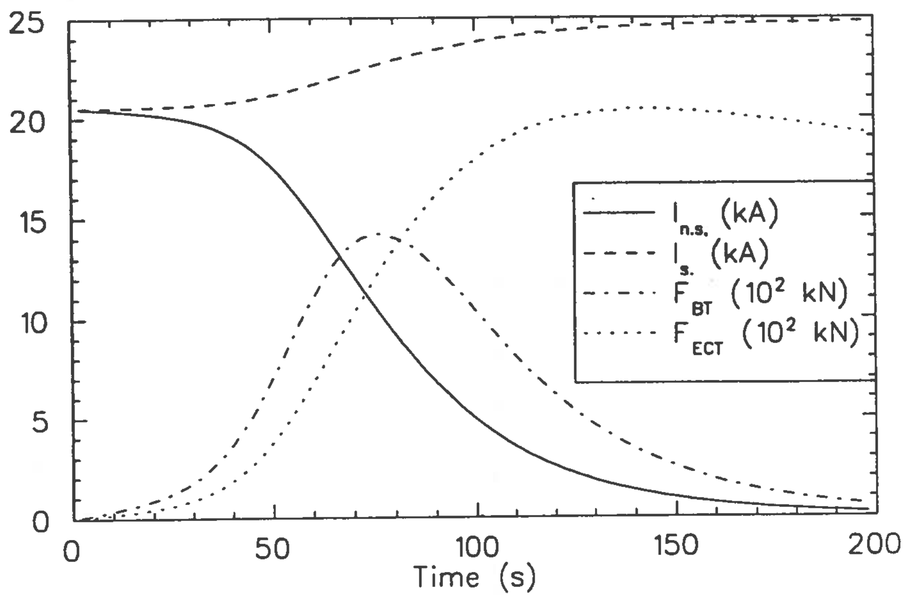

FIG. 9: Behaviour of the current in the unshorted (n.s.) and shorted (s.) BT sections and forces (absolute values) in the BT and ECT coils with a $2\,m\Omega$ dump resistor, heaters off and initial quench in the unshorted section.

Also in this case the currents and the forces maintain the characteristics shown in these figures for each short circuit configuration.

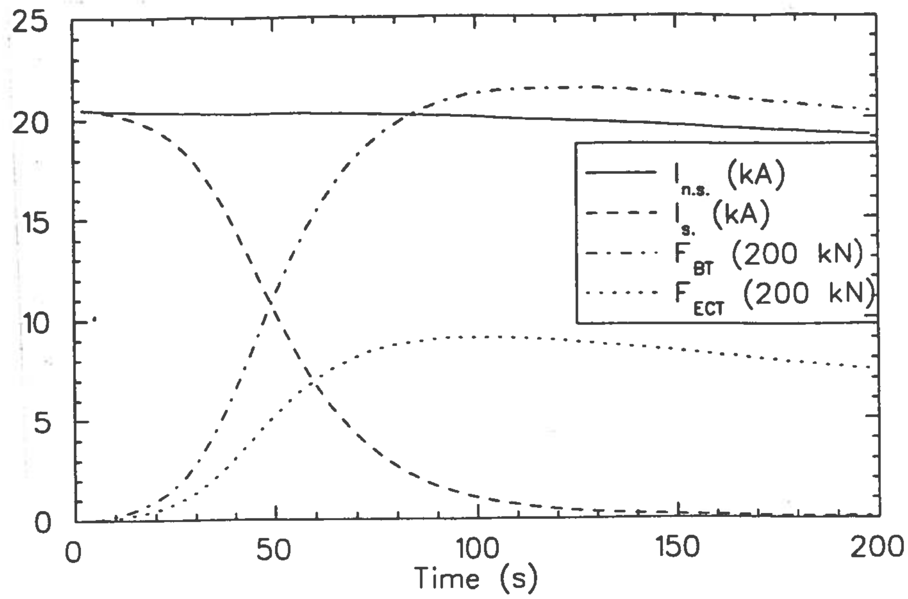

FIG. 10: Behaviour of the current in the unshorted (n.s.) and shorted (s.) BT sections and forces (absolute values) in the BT and ECT coils with a $2\,m\Omega$ dump resistor, heaters off and initial quench in the shorted section.

The maximum forces in the BT and ECT coils for the various short circuit configurations and for $2\,m\Omega$ and $20\,m\Omega$ dump resistance are reported in Table V.

Table V - Forces in the BT and ECT coils (No e.m. coupling - Heaters off)

	$2\,m\Omega$		$20\,m\Omega$	
N_{ns}-N_s	F_{BT} (kN)	F_{ECT} (kN)	F_{BT} (kN)	F_{ECT} (kN)
7-1	-4089	-2187	+1425	+2059
6-2	+5940	+3541	+5752	+3308
5-3	+6488	+4519	+6265	+4183
4-4	+6500	+4823	+6263	+4434
3-5	+6049	+4459	+5854	+4130
2-6	+5050	+3404	+4995	+3327
1-7	-2332	+1830	+1199	+2011

The decentering forces are tremendous (10-15 times the weigth of the cold mass of a single coil in the BT) and there is no difference between the highest values when the dump resistance passes from $2\,m\Omega$ to $20\,m\Omega$.

In this case it is not necessary to complete the analysis by varying the parameters of the discharge, because these forces are already not compatible with the present design of the ATLAS detector.

Therefore in order to avoid this event (short circuit and heater failure) it is necessary to have redundancy in the safety system by means, if possible, two indipendent devices.

4.3.3 Electromagnetic coupling between coils and casings

The completion of the analysis, by considering the electromagnetic coupling between coils and casings, has been carried out by means of the equation system (27-39).

The results for the different short circuit configurations (and only for the normal operation of the heaters) are listed in the Table VI.

Table VI - Forces in the BT and ECT coils (E.m. coupling - Heaters on)

	$2\,m\Omega$		$20\,m\Omega$	
N_{ns}-N_s	F_{BT} (kN)	F_{ECT} (kN)	F_{BT} (kN)	F_{ECT} (kN)
7-1	-103	-82	+487	+287
6-2	+88	-100	+614	+584
5-3	+103	-116	+831	+890
4-4	+128	+144	+1055	+1172
3-5	+163	+176	+1308	+1410
2-6	+ 229	+201	+1586	+1528
1-7	+372	+218	+1139	+1348

These data, compared with the data of Table II, show that the electromagnetic coupling between coils and casings has a large beneficial effect for the configurations with a low number of short circuited coils (a reduction of about a factor two for both the forces F_{BT} and F_{ECT}) but reduces its effect to about 10% for the configuration with 7 short circuited coils.

In case of heater failure the electromagnetic coupling between coils and casings does not change substantially the maximum forces in the BT and ECT, shown in Tables III and IV.

For this reason it is convenient to design the load bearing structure by considering the results obtained in the previous paragraph.

5 CONCLUSIONS

The analysis carried out in the previous paragraphes can be considered reasonably exsaustive because all electromagnetic and thermal processes have been considered and described with conservative assumptions.

The main results concerning the protection circuit of the BT can be summarized in the following points:

- 1) In normal conditions (heaters on) there are not substantial differences in the critical parameters of the discharge when a $20\,m\Omega$ or a $2\,m\Omega$ dump resistor is used. The only difference consists in the level of voltage at the magnet ends and in the level of energy dissipated outside the magnet. It is opinion of the authors that a $20\,m\Omega$ dump resistor represents the best solution by considering that:

  a) a voltage of 500 volts does not represent a problem for the status of art in the insulation of big magnets;

  b) the quenchback becomes effective in few seconds so that can represents an intrinsic safeguard in case of low efficiency of the heaters;

c) the energy dissipated outside the magnet is at least 30% of the stored magnetic energy so that a proportional reduction of time and cost for the magnet recovery after a fast discharge is obtained.

- 2) In the faulty conditions (heaters off) the critical parameters (maximum temperature inside the coils, maximum temperature gradient and maximum voltage) are largely different for the two values of the dump resistance. In the $2\,m\Omega$ configuration the maximum temperature inside the coil reaches the room temperature ($T_{max} = 294\,K$) with high temperature gradients and high voltages ($V_{max} \sim 1100\,V$). In the $20\,m\Omega$ configuration the maximum temperature in the coil is lower than $200\,K$ ($T_{max} = 184\,K$), also the thermal gradients are lower and the maximum voltage never exceeds $500\,V$ ($V_{max} \sim 430\,V$).

  Therefore in case of heater failure the $20\,m\Omega$ dump resistor presents for the safety of the magnet clear advantages in respect to the $2\,m\Omega$ solution. Furthermore the extracted energy is ranging from 46% (for normal or low heat exchange) to about 57% (for very bad heat exchange).

- 3) In presence of short circuit and heaters on the $2\,m\Omega$ dump resistor presents the advantages of lower decentering forces on the BT and ECT magnets. The forces are limited within 41 tons for the single coil of the BT and 34 tons for the whole ECT magnet, whereas the forces reach respectively 168 tons and 161 tons when a $20\,m\Omega$ dump resistor is used. In any case the decentering forces reach their maximum after several tens of seconds so that there is time for a protection intervention.

  When the delay between the quench start and the breaker opening (or heater firing) becomes too high ($> 10\,s$) or when there is an heater failure the forces blow up by reaching about 650 tons for the BT coil and 450 tons for the ECT magnet. These forces cannot be supported by the toroid structure so that it is necessary to have a complete assurance that this situation never happens. This will require a large redundancy in the heater and ancillary systems.

Based on these considerations the authors propose to design a protection circuit based on a $20\,m\Omega$ dump resistor (obtained as a series of two or three resistors) with a switch to pass from $20\,m\Omega$ to $2\,m\Omega$ resistance if a short circuit is detected during the fast discharge of the BT.

Fig. 11 shows the effect of the switching from $20\,m\Omega$ to $2\,m\Omega$ on the BT forces (a similar effect has been found for the ECT forces) for the short circuit configuration 1-7.

The resulting maximum decentering forces have about the same values obtained with a direct discharge on a $2\,m\Omega$ dump resistor. The detection of the short circuit and the closing of the switch must be obtained within 1 s. If the delay in this operation is 2 s the resulting forces increase of about 10%.

The short circuit detection is assured by the ground circuit (already foreseen in the present design) and by an additional device, constituted by 8 pick up coils (1000 turns and a surface of about $100\,cm^2$) positioned externally to the vacuum vessels of the BT. The induced voltages (few tens of mV) suitably amplified and compared, allow to detect the short circuit between pancakes, the number of the short circuited coils and their position. In fact the induced voltages (proportional to the current derivatives in

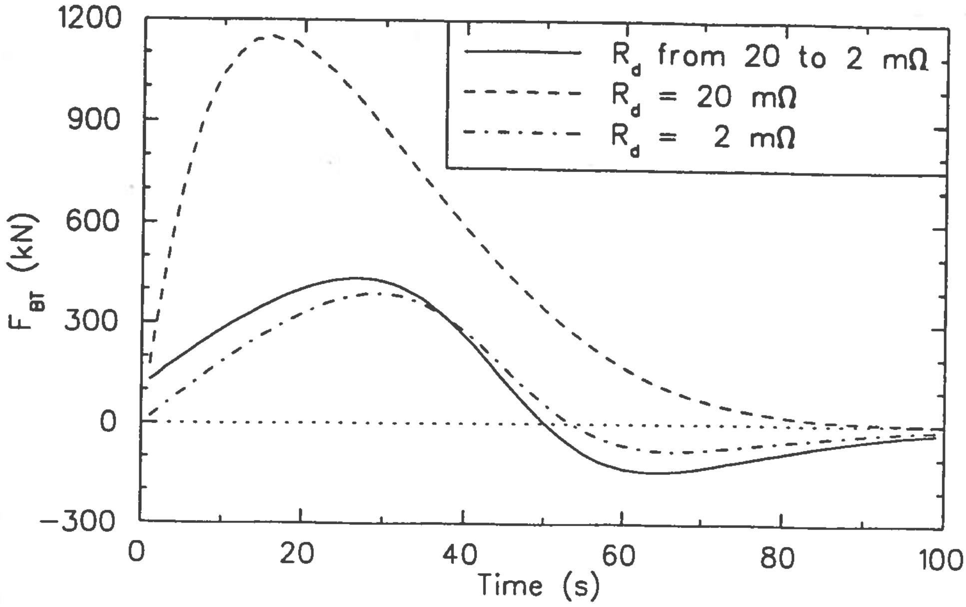

FIG. 11: Effect of the switching from $20\,m\Omega$ to $2\,m\Omega$ on the F_{BT} forces . The switch has been closed about 1 s after the breaker opening.

the coils) are very different in the pick up coils of the shorted section and in that ones of the unshorted section.

This proposal (two or three dump resistors in series with a switch) can be extended to the protection circuit of the Bo magnet .

Because the Bo magnet has a self inductance about 20 times lower than the BT the dump resistors should be respectively $1\,m\Omega$ and $0.1\,m\Omega$ in order to reproduce similar discharge rates.

The use of dump resistors in series is not necessary for the safety of Bo but it allow to simulate the switching and also to study the efficiency of the quenchback in case of heater failure with high ($1\,m\Omega$) and low ($0.1\,m\Omega$) resistances.

The improved protection system and the short circuit detection device for BT and Bo magnets are described in more details in another paper (see [4]).

REFERENCES

[1] ATLAS Barrel Toroid - Technical Design Report
CERN/LHCC/97-19 - ATLAS TDR 7 - (30/4/97)

[2] E. Acerbi et al.
Self and mutual inductances in the ATLAS Toroids
Internal Report - LASA/ATLAS/11 (29/5/97)

[3] E. Acerbi et al.
Calculation of the forces in the coils of the ATLAS Barrel Toroid and End Cap Toroids due to an unbalanced current distribution.
Internal Report - LASA/ATLAS/18 (2/9/97)

[4] E. Acerbi et al.
ATLAS Barrel Toroid supply and protection.
Internal Report - LASA/ATLAS/21 (10/10/97)

APPENDIX A

Evaluation of the quench speed.

The longitudinal speed of the quench in the present analysis is considered a free parameter, but it is necessary to define a realistic range of values for which the behaviour of the discharge is examined.

The following simple relation has been adopted:

$$v_x = (\frac{J}{c\delta})(\frac{k\rho}{\theta_c})^{1/2}G(\theta) \tag{46}$$

where:

$$G(\theta) = (\theta_m - 2\theta_c)\frac{1}{[\theta_m(\theta_m - \theta_c)]^{1/2}} \tag{47}$$

being:

J the operating current density,

δ, c, k, ρ respectively the density, the specific heat, the thermal conductivity and the resistivity of the matrix,

θ_c the difference between the critical temperature and the operating temperature,

θ_c the difference between the hot spot temperature and the operating temperature.

The function $G(\theta)$ assumes rapidly values near the unity so that the longitudinal speed in the case of the BT conductor should be taken in the following range:

$$2.3\,m/s < v_x < 3.5\,m/s \tag{48}$$

In the analysis of the discharge a larger range ($v_x(min) = 1\,m/s$ and $v_x(max) = 10\,m/s$) will be considered.

The ratios between the transverse speeds (v_y and v_z) and the longitudinal speed v_x are respectively:

$$\frac{v_y}{v_x} = (\frac{k_y}{k_x})^{1/2} \qquad \frac{v_z}{v_x} = (\frac{k_z}{k_x})^{1/2} \tag{49}$$

where k_y and k_z are the transverse thermal conductivities of the coil and k_x is the thermal conductivity of the matrix.

The transverse conductivities are given by:

$$\begin{aligned} \frac{\Delta y + w_y(is)}{k_y} &= \frac{\Delta y}{k_x} + \frac{w_y(is)}{k_{is}} + R_{12} + R_{21} \\ \frac{h_c + w_z(is)}{k_z} &= \frac{h_c}{k_x} + \frac{w_z(is)}{k_{is}} + R_{12} + R_{21} \end{aligned} \tag{50}$$

where Δy and h_c are respectively the width and the heigth of the matrix, k_{is} is the thermal conductivity of the insulation $w_y(is)$ and $w_z(is)$ are the thiknesses of the insulation between turns and between pancakes, R_{12} and R_{21} are the thermal resistances of the interfaces between the matrix and the insulation.

By assuming:

$$\begin{aligned} \Delta y &= 12\,mm & h_c &= 57\,mm \\ w_y(is) &= 0.8\,mm & w_z(is) &= 1.3\,mm \\ k_x &= 1800\,W/Km & k_{is} &= 0.1\,W/Km \\ R_{12} &= R_{21} = 5\,10^{-4}\,m^2K/W \end{aligned}$$

the transverse thermal conductivities and the speed ratios assume the values:

$$\begin{aligned} k_y &= 1.42\,W/Km & k_z &= 4.15\,W/Km \\ \frac{v_y}{v_x} &= 0.028 & \frac{v_z}{v_x} &= 0.048 \end{aligned} \tag{51}$$

APPENDIX B

Length of the quenched cable in a BT double pancake.

The quench propagates with a longitudinal speed v_x along the conductor and with speeds v_y and v_z in the transverse directions. By considering that each section of the BT coil is constituted only by two layers (double pancake) it is reasonable to assume that the propagation is developing in two separated xy planes with a delay δt given by:

$$\delta t = \frac{h}{v_z} \tag{52}$$

being h the heigth of a pancake.

At every instant the boundaries of the quenched zone in each pancake are represented by an ellipse, or arcs of ellipse and straigth lines when the quench arrives at the border of the pancake. In order to simplify the analysis, the pancake is developed along its length, the x axis is coincident with the internal border of the pancake and the y axis is located at the origin of the quench. A reduced length of the pancake will be considered:

$$L_1 = L_{panc}/N_h \tag{53}$$

being N_h the number of heaters in each double pancake of length L_{panc}.

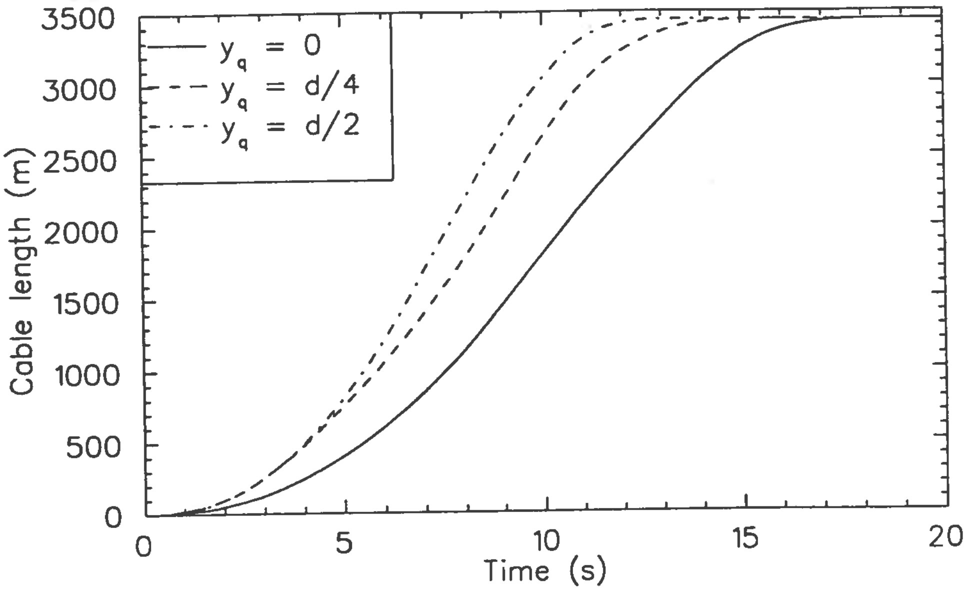

Figure B1: Quenched length of the ATLAS double pancake as a function of time and quench position for a constant quench speed ($v_x = 3m/s$).

By indicating with $x_q = 0$ and y_q the coordinates of the origin of the quench, with d the width of the pancake and with a the thickness (short side) of the insulated conductor, the length of the quenched conductor in a single pancake, at a generic instant t, depends by the boundary conditions, i.e. by the propagating length along the x axis:

$$2v_x t \leq L_1 \quad or \quad 2v_x t > L_1 \tag{54}$$

and simultaneously by the propagating length along the y axis:

$$\begin{array}{lll} v_y t < y_q & and & v_y t < (d - y_q) \\ v_y t > y_q & and & v_y t < (d - y_q) \end{array}$$

TABLE B2 - Length of the quenched conductor in a single pancake when $2v_x t > L_1$

Conditions	Length of the quenched conductor
$2v_x t > L_1$ $v_y t < y_q \quad v_y t < (d - y_q)$	$L_t = 2v_x v_y t^2[\frac{\pi}{2} + arcos(\frac{L_1}{2v_x t}) - \frac{L_1}{v_x t}[1 - (\frac{L_1}{2v_x t})^2]^{1/2}]/a$
$2v_x t > L_1$ $v_y t > y_q \quad v_y t < (d - y_q)$ $x_1 < L_1/2$	$L_t = \{v_x v_y t^2[\frac{\pi}{2} - 2arcos(\frac{L_1}{2v_x t}) + arcos(\frac{x_1}{v_x t})$ $+\frac{L_1}{v_x t}[1 - (\frac{L_1}{2v_x t})^2]^{1/2} - \frac{x_1}{v_x t}[1 - (\frac{x_1}{v_x t})^2]^{1/2}] + 2x_1 y_q\}/a$
$2v_x t > L_1$ $v_y t > y_q \quad v_y t < (d - y_q)$ $x_1 > L_1/2$	$L_t = \{v_x v_y t^2[\frac{\pi}{2} - arcos(\frac{L_1}{2v_x t})$ $+\frac{L_1}{2v_x t}[1 - (\frac{L_1}{2v_x t})^2]^{1/2}] + L_1 y_q\}/a$
$2v_x t > L_1$ $v_y t > y_q \quad v_y t > (d - y_q)$ $x_1 < L_1/2 \; x_2 < L_1/2$	$L_t = \{v_x v_y t^2[-2arcos(\frac{L_1}{2v_x t}) + arcos(\frac{x_1}{v_x t}) + arcos(\frac{x_2}{v_x t})$ $+\frac{L_1}{v_x t}[1 - (\frac{L_1}{2v_x t})^2]^{1/2} - \frac{x_1}{v_x t}[1 - (\frac{x_1}{v_x t})^2]^{1/2}$ $-\frac{x_2}{v_x t}[1 - (\frac{x_2}{v_x t})^2]^{1/2}] + 2x_1 y_q + 2x_2(d - y_q)\}/a$
$2v_x t > L_1$ $v_y t > y_q \quad v_y t > (d - y_q)$ $x_1 > L_1/2 \; x_2 < L_1/2$	$L_t = \{v_x v_y t^2[-arcos(\frac{L_1}{2v_x t}) + arcos(\frac{x_2}{v_x t})$ $+\frac{L_1}{2v_x t}[1 - (\frac{L_1}{2v_x t})^2]^{1/2} - \frac{x_2}{v_x t}[1 - (\frac{x_2}{v_x t})^2]^{1/2}]$ $+L_1 y_q + 2x_2(d - y_q)\}/a$
$2v_x t > L_1$ $v_y t > y_q \quad v_y t > (d - y_q)$ $x_1 < L_1/2 \; x_2 > L_1/2$	$L_t = \{v_x v_y t^2[-arcos(\frac{L_1}{2v_x t}) + arcos(\frac{x_1}{v_x t})$ $+\frac{L_1}{2v_x t}[1 - (\frac{L_1}{2v_x t})^2]^{1/2} - \frac{x_1}{v_x t}[1 - (\frac{x_1}{v_x t})^2]^{1/2}]$ $+L_1(d - y_q) + 2x_1 y_q\}/a$
$2v_x t > L_1$ $v_y t > y_q \quad v_y t > (d - y_q)$ $x_1 > L_1/2 \; x_2 > L_1/2$	$L_t = L_1 d/a$
For x_1 and x_2 see note of Table B1	

For the analysis of the coil protection, in order to have the most conservative results, the origin of the quench will be put at $y_q = 0$ during a normal discharge of the coil whereas it will be put at $y_q = d/2$ during a faulty discharge.

$$
\begin{array}{lllll}
v_y t & < & y_q & and & v_y t > (d - y_q) \\
v_y t & > & y_q & and & v_y t > (d - y_q)
\end{array}
\tag{55}
$$

TABLE B1 - Length of the quenched conductor in a single pancake when $2v_x t \leq L_1$

Conditions	Length of the quenched conductor
$2v_x t \leq L_1$ $v_y t < y_q \quad v_y t < (d - y_q)$	$L_t = \pi v_x v_y t^2 / a$
$2v_x t \leq L_1$ $v_y t > y_q \quad v_y t < (d - y_q)$ for x_1 see **	$L_t = \{v_x v_y t^2 [\frac{\pi}{2} + arcos(\frac{x_1}{v_x t})$ $- \frac{x_1}{v_x t}[1 - (\frac{x_1}{v_x t})^2]^{1/2}] + 2x_1 y_q\}/a$
$2v_x t \leq L_1$ $v_y t < y_q \quad v_y t > (d - y_q)$ For x_2 see **	$L_t = \{v_x v_y t^2 [\frac{\pi}{2} + arcos(\frac{x_2}{v_x t})$ $- \frac{x_2}{v_x t}[1 - (\frac{x_2}{v_x t})^2]^{1/2}] + 2x_2(d - y_q)\}/a$
$\mathbf{2v_x t \leq L_1}$ $v_y t > y_q \quad v_y t > (d - y_q)$ For x_1,x_2 see **	$L_t = \{v_x v_y t^2 [arcos(\frac{x_1}{v_x t}) + arcos(\frac{x_2}{v_x t})$ $- \frac{x_1}{v_x t}[1 - (\frac{x_1}{v_x t})^2]^{1/2} - \frac{x_2}{v_x t}[1 - (\frac{x_2}{v_x t})^2]^{1/2}]$ $+ 2x_1 y_q + 2x_2(d - y_q)\}/a$
** $\quad x_1 = v_x(t^2 - y_q^2/v_y^2)^{1/2}$	$x_2 = v_x(t^2 - (d - y_q)^2/v_y^2)^{1/2}$

When the ellipse is inside the x and y boundaries ($2v_x t \leq L_1$ and $v_y t < y_q$ and $v_y t < (d - y_q)$) the quenched length in a single pancake is given by:

$$L_{t1} = \pi v_x v_y t^2 / a \tag{56}$$

whereas when the ellipse covers completely the pancake surface ($2v_x t > L_1$ and $v_x(t^2 - y_q^2/v_y^2)^{1/2} > L_1/2$ and $v_x(t^2 - (d - y_q)^2/v_y^2)^{1/2} > L_1/2$) the quenched length of the single pancake is simple given by:

$$L_{t1} = L_1(d/a) \tag{57}$$

The quenched lengths in the intermediate situations are reported in Tables B1 (when $2v_x t \leq L_1$) and B2 (when $2v_x t > L_1$).

The total quenched length L_t^* in the double pancake is given by:

$$L_t^* = (L_{t1} + L_{t2}) N_h \tag{58}$$

being L_{t1} and L_{t2} respectively the quenched lengths (calculated with the formulas reported in table B1) of the first (origin of the quench) and second pancake.

The evolution of the quenched length in a double pancake of the ATLAS coil for different positions of the quench origin (different values of y_q) is shown in Fig. B1. The reaching of the boundary limits by the quench is revealed by changes in the curve slope, the time required for a complete quench of the double pancake is maximum when $y_q = 0$ or $y_q = d$ (i.e. when the the origin of the quench is located at the coil boundaries).

As shown in Fig. B1, with a quench speed $v_x = 3\,m/s$, the total transition to the resistive state of a double pancake requires about 12 - 18 s (depending by the position y_q of the quench).

APPENDIX C

Summary of the discharge parameters (normal operation and heater failure).

TABLE C1
Normal operation: $I_{max} = 20500\,A$, normal heat exchange between coil and casing, heaters on, 1 heater/double pancake.
$V_{max} = rI_1 + L_1(dI_1/dt) + M_{12}(dI_2/dt)$

$R(dump)$ (Ω)	v_x (m/s)	T_{max} (K)	V_{max} (V)	I_1 (A)	Δt (s)	I_{2m} (A)	ΔT (K)	ϵ
0.0002	1.0	79.8	69.4	20445.4	8.2	107733.4	36.1	0.996
0.0005	1.0	79.7	62.9	20433.1	8.2	107118.2	35.9	0.990
0.0010	1.0	79.4	52.1	20412.8	8.2	106100.0	35.7	0.980
0.0020	1.0	78.8	-42.0	20155.9	8.2	104079.2	35.2	0.960
0.0050	1.0	76.9	-106.9	19673.1	8.1	98067.6	33.7	0.900
0.0100	1.0	73.9	-211.5	19290.2	7.8	88712.4	31.2	0.805
0.0200	1.0	67.7	-411.0	19787.7	6.9	73020.5	26.2	0.631
0.0002	3.0	79.3	33.4	20425.1	4.6	104649.6	35.4	0.996
0.0005	3.0	79.1	27.1	20417.4	4.6	104071.5	35.3	0.990
0.0010	3.0	78.8	-20.2	20199.3	4.6	103111.9	35.1	0.981
0.0020	3.0	78.2	-41.6	20036.2	4.6	101193.9	34.6	0.961
0.0050	3.0	76.4	-105.6	19600.1	4.5	95557.8	33.1	0.903
0.0100	3.0	73.5	-209.2	19327.7	4.5	86836.3	30.7	0.810
0.0200	3.0	67.5	-408.3	19881.9	4.2	72162.5	25.9	0.640
0.0002	10.0	79.1	6.4	15675.1	2.9	103900.4	35.3	0.996
0.0005	10.0	79.0	-9.8	20439.3	2.9	103331.2	35.2	0.991
0.0010	10.0	78.7	-20.1	20146.8	2.9	102387.2	34.9	0.981
0.0020	10.0	78.1	-41.4	19980.1	2.9	100495.7	34.4	0.961
0.0050	10.0	76.3	-105.1	19563.1	2.9	94967.9	33.0	0.904
0.0100	10.0	73.4	-208.4	19299.2	2.9	86402.9	30.6	0.812
0.0200	10.0	67.5	-407.1	19735.4	2.8	72013.7	25.9	0.643

TABLE C2

Normal operation: $I_{max} = 20500\,A$, low heat exchange between coil and casing, heaters on, 1 heater/double pancake.

$V_{max} = rI_1 + L_1(dI_1/dt) + M_{12}(dI_2/dt)$

$R(dump)$ (Ω)	v_x (m/s)	T_{max} (K)	V_{max} (V)	I_1 (A)	Δt (s)	I_{2m} (A)	ΔT (K)	ϵ
0.0002	1.0	84.2	36.0	20155.2	17.5	120916.7	47.1	0.997
0.0005	1.0	84.0	29.6	20098.2	17.4	120331.6	47.0	0.991
0.0010	1.0	83.8	-20.4	20487.4	17.4	119392.5	46.8	0.982
0.0020	1.0	83.2	-41.7	20305.5	17.3	117516.4	46.3	0.964
0.0050	1.0	81.6	-106.3	19971.0	17.0	112064.2	45.1	0.911
0.0100	1.0	79.0	-211.5	19588.4	16.1	103361.5	42.9	0.826
0.0200	1.0	73.6	-411.6	19418.9	13.5	87994.1	38.5	0.669
0.0002	3.0	82.8	7.8	15856.2	11.9	113190.5	45.9	0.997
0.0005	3.0	82.7	-9.3	20280.8	11.9	112665.1	45.8	0.991
0.0010	3.0	82.4	-20.0	20260.9	11.9	111797.6	45.6	0.982
0.0020	3.0	81.9	-41.2	20180.1	11.9	110081.4	45.2	0.965
0.0050	3.0	80.3	-104.7	19811.4	11.7	105075.5	43.9	0.912
0.0100	3.0	77.7	-208.2	19534.3	11.3	97074.6	41.7	0.828
0.0200	3.0	72.5	-408.1	19488.8	10.1	83250.9	37.4	0.674
0.0002	10.0	82.6	7.7	15785.5	10.1	112046.0	45.7	0.997
0.0005	10.0	82.5	-9.7	20439.1	10.1	111524.5	45.6	0.991
0.0010	10.0	82.2	-20.0	20433.4	10.1	110662.2	45.4	0.982
0.0020	10.0	81.7	-41.0	20104.2	10.1	108958.6	45.0	0.965
0.0050	10.0	80.1	-104.3	19730.4	9.9	103979.6	43.7	0.912
0.0100	10.0	77.5	-207.4	19480.8	9.5	96030.4	41.6	0.829
0.0200	10.0	72.3	-406.8	19817.7	8.6	82328.5	37.2	0.675

TABLE C3

Normal operation: $I_{max} = 20500\,A$, no heat exchange between coil and casing, heaters on, 1 heater/double pancake.

$V_{max} = rI_1 + L_1(dI_1/dt) + M_{12}(dI_2/dt)$

$R(dump)$ (Ω)	v_x (m/s)	T_{max} (K)	V_{max} (V)	I_1 (A)	Δt (s)	I_{2m} (A)	ΔT (K)	ϵ
0.0002	1.0	85.8	15.0	18460.3	∞	125250.8	53.1	0.997
0.0005	1.0	85.7	-10.1	20497.9	∞	124693.3	53.0	0.991
0.0010	1.0	85.4	-20.4	20488.0	∞	123772.4	52.8	0.983
0.0020	1.0	84.9	-41.6	20323.3	∞	121951.3	52.4	0.965
0.0050	1.0	83.4	-106.0	20007.9	∞	116647.8	51.3	0.914
0.0100	1.0	80.9	-211.1	19634.3	∞	108287.8	49.4	0.831
0.0200	1.0	75.8	-411.5	19446.3	∞	93385.3	45.4	0.679
0.0002	3.0	84.3	8.3	15835.4	∞	116197.6	52.2	0.997
0.0005	3.0	84.1	-9.2	20275.9	∞	115690.1	52.1	0.992
0.0010	3.0	83.9	-19.8	20256.0	∞	114848.0	51.9	0.983
0.0020	3.0	83.4	-41.0	20216.4	∞	113184.6	51.6	0.966
0.0050	3.0	81.9	-104.4	19858.2	∞	108336.0	50.4	0.915
0.0100	3.0	79.4	-207.9	19605.6	∞	100589.5	48.5	0.834
0.0200	3.0	74.5	-408.0	19520.2	∞	86999.6	44.5	0.684
0.0002	10.0	84.0	8.1	15847.0	∞	115023.4	52.1	0.997
0.0005	10.0	83.9	-9.7	20439.0	∞	114516.7	52.0	0.992
0.0010	10.0	83.7	-20.0	20433.3	∞	113679.4	51.8	0.983
0.0020	10.0	83.2	-40.9	20143.7	∞	112024.5	51.5	0.966
0.0050	10.0	81.7	-104.0	19776.9	∞	107199.2	50.3	0.915
0.0100	10.0	79.2	-207.1	19533.1	∞	99483.4	48.4	0.834
0.0200	10.0	74.2	-406.7	19860.2	∞	85990.9	44.4	0.685

TABLE C4

Faulty condition: $I_{max} = 20500\,A$, heater failure, quench only in a double pancake, normal heat exchange between coil and casing, quenchback.

$V_{max} = rI_1 + L_1(dI_1/dt) + M_{12}(dI_2/dt)$

$R(dump)$ (Ω)	v_x (m/s)	T_{max} (K)	V_{max} (V)	I_1 (A)	Δt (s)	I_{2m} (A)	ΔT (K)	ϵ
0.0002	1.0	206.4	674.4	12864.7	10.2	80006.2	140.0	0.994
0.0005	1.0	205.1	664.7	11812.1	10.2	79330.4	138.8	0.984
0.0010	1.0	202.7	648.1	12731.6	10.2	78214.1	136.8	0.967
0.0020	1.0	197.9	614.4	12564.1	10.2	76031.5	132.5	0.933
0.0050	1.0	182.5	511.1	12055.5	10.1	69961.8	118.9	0.834
0.0100	1.0	147.7	302.6	11484.9	9.6	63815.1	89.8	0.698
0.0200	1.0	88.3	-58.9	19288.3	8.1	59191.4	42.4	0.545
0.0002	3.0	196.0	603.8	12754.0	6.0	80213.9	129.8	0.994
0.0005	3.0	194.8	595.3	12729.2	6.0	79570.1	128.7	0.984
0.0010	3.0	192.7	580.8	12645.3	6.0	78507.5	126.9	0.968
0.0020	3.0	188.2	549.6	12486.1	5.9	76444.3	122.8	0.935
0.0050	3.0	174.5	460.2	12001.3	5.9	70664.0	111.0	0.841
0.0100	3.0	144.1	280.4	11431.3	5.8	64646.2	85.7	0.707
0.0200	3.0	89.4	-52.7	19247.7	5.3	59555.8	42.6	0.550
0.0002	10.0	191.2	570.7	12729.4	4.0	80283.2	125.0	0.994
0.0005	10.0	190.0	562.8	12673.6	4.0	79655.2	123.9	0.985
0.0010	10.0	188.0	548.8	12585.6	4.0	78622.8	122.2	0.969
0.0020	10.0	183.9	521.3	12437.7	4.0	76600.5	118.6	0.936
0.0050	10.0	170.8	437.1	11973.0	4.0	70962.0	107.3	0.843
0.0100	10.0	142.2	269.4	11387.0	3.9	64952.4	83.7	0.712
0.0200	10.0	89.9	-52.7	19248.6	3.7	59785.3	42.6	0.553

TABLE C5

Faulty condition: $I_{max} = 20500\,A$, heater failure, quench only in a double pancake, low heat exchange between coil and casing, quenchback.

$R(dump)$ (Ω)	v_x (m/s)	T_{max} (K)	V_{max} (V)	I_1 (A)	Δt (s)	I_{2m} (A)	ΔT (K)	ϵ
0.0002	1.0	256.2	941.3	12956.1	21.5	81635.0	206.5	0.994
0.0005	1.0	254.4	928.3	12892.6	21.5	81009.3	204.8	0.984
0.0010	1.0	251.4	907.0	12798.6	21.5	79939.5	202.0	0.968
0.0020	1.0	245.2	862.8	12656.0	21.4	77887.0	196.1	0.934
0.0050	1.0	225.6	729.7	12169.2	21.0	72267.5	177.7	0.839
0.0100	1.0	186.1	487.7	11610.1	19.6	66515.6	141.3	0.704
0.0200	1.0	115.6	107.7	10091.9	15.3	63286.2	77.3	0.543
0.0002	3.0	241.4	847.0	12903.4	15.3	83243.3	191.9	0.994
0.0005	3.0	239.9	836.0	12872.9	15.3	82603.2	190.4	0.985
0.0010	3.0	237.3	817.3	12779.2	15.3	81546.5	188.0	0.968
0.0020	3.0	231.9	779.4	12644.2	15.3	79489.8	182.9	0.936
0.0050	3.0	214.6	662.7	12199.9	15.1	73783.1	166.7	0.843
0.0100	3.0	179.0	446.6	11639.0	14.4	67655.7	134.0	0.711
0.0200	3.0	114.3	100.4	10051.6	12.3	63511.5	75.6	0.547
0.0002	10.0	237.1	819.5	12905.3	13.7	83567.1	187.6	0.994
0.0005	10.0	235.7	808.9	12844.4	13.7	82930.4	186.2	0.985
0.0010	10.0	233.1	790.5	12777.9	13.7	81887.6	183.8	0.969
0.0020	10.0	227.9	754.0	12613.4	13.7	79842.8	178.9	0.937
0.0050	10.0	211.2	641.8	12173.0	13.5	74216.5	163.3	0.844
0.0100	10.0	176.7	433.5	11653.7	12.9	68035.4	131.7	0.713
0.0200	10.0	113.8	97.7	10053.3	11.2	63649.2	75.1	0.548

TABLE C6

Faulty condition: $I_{max} = 20500\,A$, heater failure, quench only in a double pancake, no heat exchange between coil and casing, no quenchback.

$V_{max} = rI_1 + L_1(dI_1/dt) + M_{12}(dI_2/dt)$

$R(dump)$ (Ω)	v_x (m/s)	T_{max} (K)	V_{max} (V)	I_1 (A)	Δt (s)	I_{2m} (A)	ΔT (K)	ϵ
0.0020	1.0	294.0	1083.7	12422.6	∞	70407.5	265.7	0.932
0.0050	1.0	273.9	950.6	11957.3	∞	65329.1	246.1	0.831
0.0100	1.0	242.3	747.9	11017.7	∞	57338.5	215.4	0.678
0.0200	1.0	187.1	430.6	9643.7	∞	45472.2	161.5	0.427
0.0020	3.0	293.3	1078.5	12394.7	∞	70078.6	265.0	0.932
0.0050	3.0	273.2	945.9	11953.9	∞	65018.7	245.5	0.831
0.0100	3.0	241.6	743.7	11014.2	∞	57056.8	214.8	0.678
0.0200	3.0	186.6	427.8	9621.7	∞	45258.6	161.0	0.428
0.0020	10.0	293.2	1077.9	12374.0	∞	70037.3	264.9	0.932
0.0050	10.0	273.1	945.3	11934.8	∞	64977.0	245.4	0.831
0.0100	10.0	241.6	743.2	10997.6	∞	57017.7	214.8	0.678
0.0200	10.0	186.6	427.4	9623.9	∞	45225.5	160.9	0.428